J Chem Crystallogr (2014) 44:506–511
DOI 10.1007/s10870-014-0541-3

ORIGINAL PAPER

Synthesis, Structural and Spectroscopic Characterization of a New Coordination Polymer Based on a Tetraiminodiphenolate Macrocycle and Piperazine: $[\{Cu_2(tidf)(\mu\text{-}ppz)\}(ClO_4)_2]_n$

Renan Nakamura de Jesus · Marcos A. Ribeiro · Mayara H. Inoue · Fábio Souza Nunes · Rafael Block Samulewski

Received: 17 June 2014 / Accepted: 22 August 2014 / Published online: 7 September 2014

Abstract Herein we report on the synthesis, single crystal X-ray structure and spectroscopic properties of $[\{Cu_2(tidf)(\mu\text{-}ppz)\}(ClO_4)_2]_n$ (tidf = a Robson-type macrocyclic ligand obtained by condensation of 2,6-diformyl-4-methylphenol and 1,3–diaminopropane). The two copper(II) centers in the dicopper(II,II) chromophore share identical coordination environment. The geometry around the copper(II) is square pyramidal and has $[Cu_2(tidf)]^{2+}$ units bridged by piperazine and forming a 1D–coordination polymer. The structure is also supported by non-classic hydrogen bonding such as $C\text{–}H\cdots O_{perchlorate}$. Electronic spectroscopy agrees with the C_{4v} micro-symmetry around the metal center as ligand-field transitions are splitted when compared to the spectrum of the parent complex $[Cu_2(tidf)(ClO_4)_2(H_2O)_2]$.

Keywords Coordination polymer · Dicopper(II) · Tetraiminodiphenolate · Macrocycle piperazine · Crystal structure

Introduction

A considerable part of the coordination chemistry has been centered on the use of metal ions as template of cyclization reactions to produce macrocycle ligands [1–5]. Robson-type ligands, obtained from condensation of 2,6-diformyl-4-methylphenol and diamines, have been investigated over the years as their coordination compounds show interesting magnetic, redox and structural properties [6–20]. This category of macrocycle is appealing because it can bind two metal ions simultaneously allowing the preparation of homometallic and heterometallic compounds. In addition, there is always the possibility to occupy the axial positions of the related complexes with ambidentate ligands and obtain high nuclearity systems exhibiting unusual molecular architectures [21–23].

Earlier, we report three heteropolynuclear metal complexes of the Robson family. Results show a very interesting case of self-assembly of building molecules into extended structures in the solid state [7]. In this work, continuing our general interest in the synthesis of metal complexes of the tetraminodiphenolate macrocycle ligand (Scheme 1), we report the preparation and characterization of a new coordination polymer based on a dicopper macrocycle complex and piperazine as building blocks.

Experimental Section

Reagent grade chemicals were used in this work. $[Cu_2(tidf)(ClO_4)_2(H_2O)_2]$ was prepared as described elsewhere [24].

The macrocyclic ligand tidf was prepared by the condensation of 2,6-diformyl-4-methylphenol and 1,3-diaminopropane by a template reaction with magnesium acetate and magnesium nitrate according to the procedure of Nag and co-workers [25]. The magnesium complex $[Mg_2(tidf)](NO_3)_2\cdot 4H_2O$ was used to prepare the binuclear compound $[Cu_2(tidf)(ClO_4)_2(H_2O)_2]$ through a transmetallation reaction as described by Mandal et al. [24]. Reaction

---

R. N. de Jesus · R. B. Samulewski
Universidade Tecnológica Federal do Paraná, Câmpus Apucarana, Rua Marcílio Dias, n°635, Jardim Paraíso, Apucarana, PR 86812-460, Brazil

M. A. Ribeiro · M. H. Inoue · F. S. Nunes (✉)
Departamento de Química, Universidade Federal do Paraná, Cx. Postal 19081, Curitiba, PR 81531-980, Brazil
e-mail: fsnunes@ufpr.br

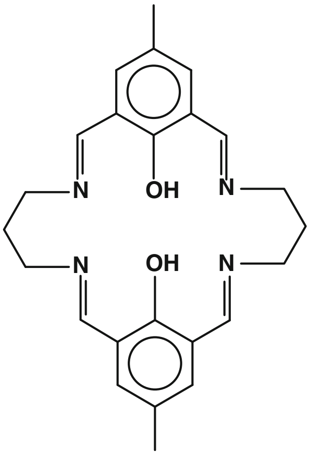

Scheme 1 Ligand tidf

with piperazine in a 1:1 molar ratio produced the polymeric complex [{Cu_2(tidf)(μ-ppz)}$(ClO_4)_2$]$_n$, which was characterized structurally and spectroscopically as described below.

Synthesis

[{Cu_2(tidf)(μ-ppz)}$(ClO_4)_2$]$_n$

Piperazine (56 mg, 0.65 mmol) was dissolved in 10 mL of distilled water and then 5 mL of isopropanol was added very slowly to form a new layer. After, a solution containing 0.5 g (0.65 mmol) of [Cu_2(tidf)$(ClO_4)_2(H_2O)_2$] in 15 mL of acetonitrile was slowly poured to the bi-layered water/isopropanol mixture and the system was keep still for the diffusion of the solvents. Small dark-green crystals, suitable for X ray crystallography were then isolated, washed with methanol, acetonitrile, diethylether and dried under vacuum. The yield was 200 mg (38 %). $C_{28}H_{36}Cl_2Cu_2N_6O_{10}$: C, 41.28; H, 4.45; N, 10.32 %. Found: C, 40.82; H, 4.25; N, 10.07 %.

Physical Measurements

UV–visible spectra in the range 190–900 nm were obtained on a VARIAN Cary 100 spectrophotometer in the solid state by diffuse reflectance with a Labsphere® integration sphere. Infrared spectra were obtained with a FTS3500GX Bio-Rad Excalibur series spectrophotometer in the region 4,000–400 cm^{-1} in KBr pellets. Elemental analyses were performed on a Perkin–Elmer CHN 2400 analyzer.

Structural Determination and Refinement

A Bruker D8 VENTURE PHOTON diffractometer operated using graphite monochromator and Mo-Kα radiation (λ = 0.71073 Å) was used for the X-ray structure analyses. The crystal structure was solved by direct methods with SHELXS2013 [26]. The final structure was refined with SHELXL2013 [26] with anisotropic displacement parameters for all non-hydrogen atoms; hydrogen atoms were refined isotropically as riding atoms at their theoretical ideal positions [27]. Drawings were made with Olex2 [28]. More detailed information about the structure determinations is given in Table 1.

Table 1 Crystal data and structure refinement for [{Cu_2(tidf)(μ-ppz)}$(ClO_4)_2$]$_n$

Empirical formula	$C_{14}H_{17}ClCuN_3O_5$	
Formula weight	406.30	
Temperature	293 K	
Wavelength	0.71073 Å	
Crystal system	Monoclinic	
Space group	$P2_1/c$	
Unit cell dimensions	a = 17.749 (5) Å	β = 144.009(5)°
	b = 8.573(5) Å	
	c = 18.271(5) Å	
Volume	1,633.8(12) $Å^3$	
Z	4	
Density (calculated)	1.652 Mg/m^3	
Absorption coefficient	1.53 mm^{-1}	
F(000)	832	
Crystal size	0.63 × 0.19 × 0.15 mm^3	
Theta range for data collection	3.1–33.9°	
Index ranges	$-22 \leq h \leq 22$, $-10 \leq k \leq 10$, $-22 \leq l \leq 22$	
Reflections collected	54,527	
Independent reflection	3,343	
Independent reflections with $I > 2\sigma(I)$	3,098 [R(int) = 0.026]	
Refinement method	Full-matrix least-squares on F^2	
Data/restraints/parameters	3343/178/223	
Goodness-of-fit on F^2	1.103	
Final R indices [$I > 2\sigma(F^2)$]	R1 = 0.0420, $wR(F^2)$ = 0.1127	
R indices (all data)	0.0420	
Extinction coefficient	0.0038(8)	
Largest diff. peak and hole	1.14 and −0.86 $e.Å^{-3}$	

$w = 1/[\sigma^2(F_o^2) + (0.052P)^2 + 3.4888P]$ where $P = (F_o^2 + 2F_c^2)/3$

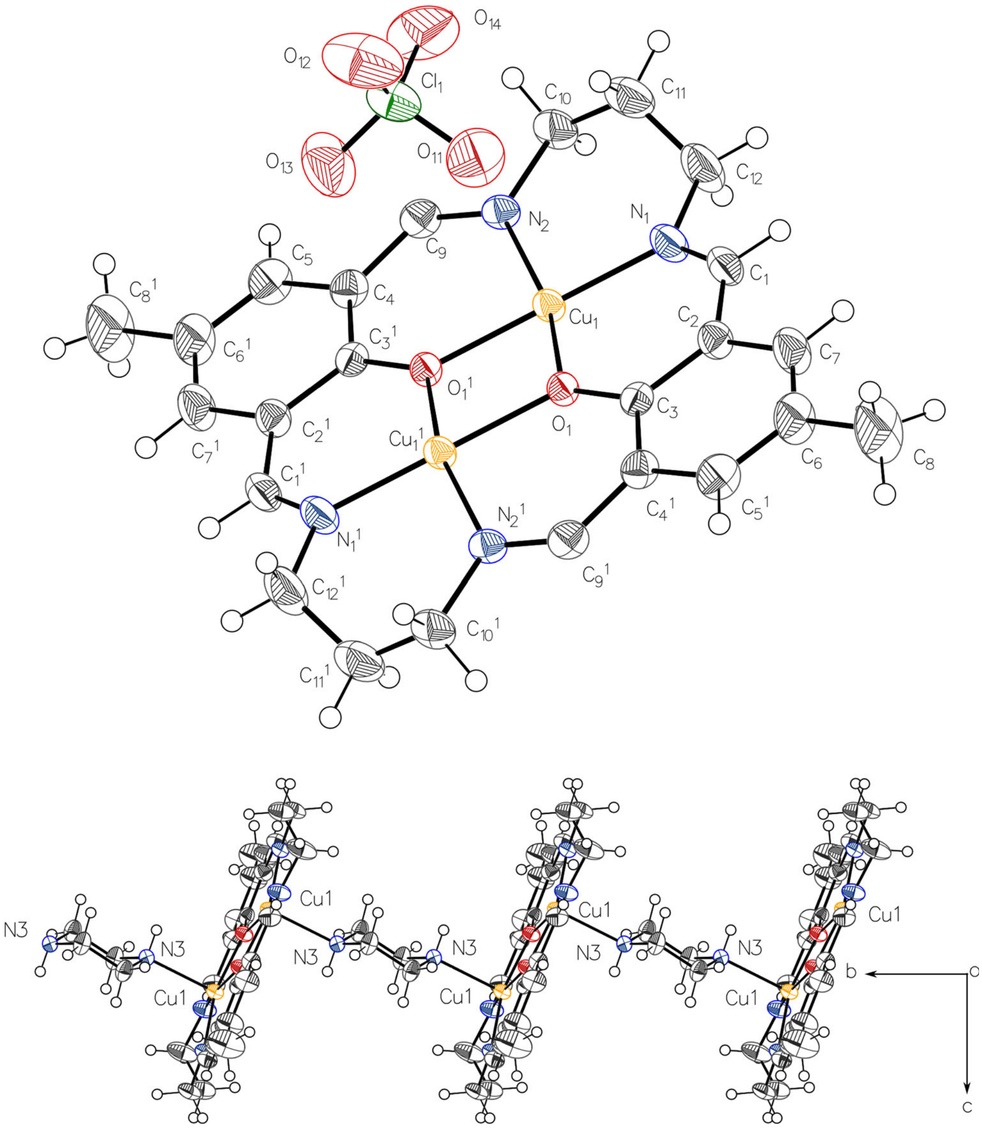

Fig. 1 (*Top*) view of $[\{Cu_2(tidf)(\mu\text{-}ppz)\}(ClO_4)_2]_n$ projection showing the atom-numbering scheme. Atom displacement ellipsoids were drawn at the 50 % probability level. (*Bottom*) view of the extended 1D chain structure along the crystallographic axis *a*

Results and Discussion

Structural Description

The complex $[\{Cu_2(tidf)(\mu\text{-}ppz)\}(ClO_4)_2]_n$ crystallizes in the monoclinic space group $P2_1/c$. Figure 1 shows the projection of the molecular structure where the copper(II) ions experiences a square pyramidal geometry. Each macrocyclic ligand (tidf) binds two metal centers in the equatorial plane through four imines and two phenolate groups, while the axial site is occupied by a piperazine ligand that bridges two units of $[Cu_2(tidf)]^{2+}$. The copper(II) ions are out of the equatorial plane, as indicated by the mean deviations from the least-square planes N1N2O1O1^i ($i = -x, -y + 1, -z-1$) at 0.2040(12) Å. The shortest Cu–Cu^i distance is 3.1521(11) Å. The Cu-piperazine bond distance, Cu1–N3 at 2.312(3) Å, is significantly longer than the equatorial bond lengths (Cu1–N1 1.969(3) Å, Cu1–N2 1.987(3) Å and Cu1–O1 2.007(19) Å), which is a clear evidence of the tetragonal distortion expected for a d^9 ion. Some main angles are N1-Cu1–N2 96.73(12)°, N1–Cu1–O1 92.10(10)°, O1–Cu1–O1^i 75.75(9)°, N1–Cu1–N3 97.49(11)° and O1^i–Cu1–N2 93.04(10)°. Other bond distances and angles are listed in Table 2.

Mandal and co-workers [24] reported the crystal structure of the dicopper complex $[Cu_2(tidf)(ClO_4)_2(H_2O)_2]$. It crystallizes in the monoclinic space group $P2_1/a$ and the structure has two different molecules in the unit cell, one pseudooctahedral and the other square-pyramidal. Bond distances reported for the hexa-coordinated copper are Cu1–O(H_2O) at 2.451 (9) Å, Cu1–O(ClO_4) at 2.589 (10), Cu1–O(phenolate) at 1.981(6) Å and Cu1–N at 1.956(8). In the second molecule, the copper(II) is axially bound to a water molecule (Cu2–O(H_2O) = 2.451(6) Å) and

Table 2 Selected bond lengths/Å and angles/° for $[\{Cu_2(tidf)(\mu\text{-}ppz)\}(ClO_4)_2]_n$

Cu1—O1^{i}	1.9864 (19)	C5—C4	1.403 (4)
Cu1—O1	2.0070 (19)	C5—C6^{i}	1.369 (5)
Cu1—N2	1.987 (2)	C4—C3^{i}	1.416 (4)
Cu1—N3	2.312 (3)	C4—C9	1.446 (4)
Cu1—N1	1.969 (3)	C2—C1	1.446 (5)
Cl1—O14	1.400 (3)	C2—C7	1.409 (4)
Cl1—O13	1.404 (3)	C1—H1	0.9300
Cl1—O11	1.462 (4)	C13—H13A	0.9700
Cl1—O12	1.404 (4)	C13—H13B	0.9700
O1—Cu1^{i}	1.9863 (19)	C12—H12A	0.9700
O1—C3	1.326 (3)	C12—H12B	0.9700
N2—C9	1.272 (4)	C12—C11	1.474 (6)
N2—C10	1.488 (4)	C10—H10A	0.9700
N3—C14^{ii}	1.471 (4)	C10—H10B	0.9700
N3—C13	1.467 (4)	C10—C11	1.499 (5)
N3—H3	0.878 (18)	C7—H7	0.9300
N1—C1	1.278 (4)	C7—C6	1.375 (5)
N1—C12	1.486 (4)	C6—C5^{i}	1.369 (5)
C14—N3^{ii}	1.471 (4)	C6—C8	1.522 (5)
C14—H14A	0.9700	C11—H11A	0.9700
C14—H14B	0.9700	C11—H11B	0.9700
C14—C13	1.520 (4)	C8—H8A	0.9600
C3—C4^{i}	1.416 (4)	C8—H8B	0.9600
C3—C2	1.410 (4)	C8—H8C	0.9600
C5—H5	0.9300		
O1^{i}—Cu1—O1	75.75 (9)	C5—C4—C9	115.5 (3)
O1^{i}—Cu1—N2	93.04 (10)	C3—C2—C1	124.7 (3)
O1^{i}—Cu1—N3	91.71 (9)	C7—C2—C3	120.2 (3)
O1—Cu1—N3	92.47 (9)	C7—C2—C1	115.2 (3)
N2—Cu1—O1	163.08 (9)	N1—C1—C2	128.6 (3)
N2—Cu1—N3	100.61 (10)	N1—C1—H1	115.7
N1—Cu1—O1^{i}	165.11 (10)	C2—C1—H1	115.7
N1—Cu1—O1	92.10 (10)	N3—C13—C14	113.4 (3)
N1—Cu1—N2	96.73 (12)	N3—C13—H13A	108.9
N1—Cu1—N3	97.49 (11)	N3—C13—H13B	108.9
O14—Cl1—O13	113.9 (3)	C14—C13—H13A	108.9
O14—Cl1—O11	107.0 (2)	C14—C13—H13B	108.9
O14—Cl1—O12	112.2 (2)	H13A—C13—H13B	107.7
O13—Cl1—O11	104.5 (2)	N2—C9—C4	128.9 (3)
O12—Cl1—O13	111.8 (3)	N1—C12—H12A	109.3
O12—Cl1—O11	106.6 (3)	N1—C12—H12B	109.3
Cu1^{i}—O1—Cu1	104.25 (9)	H12A—C12—H12B	108.0
C3—O1—Cu1^{i}	127.59 (17)	C11—C12—N1	111.6 (3)
C3—O1—Cu1	128.16 (17)	C11—C12—H12A	109.3
C9—N2—Cu1	122.6 (2)	C11—C12—H12B	109.3
C9—N2—C10	113.8 (3)	N2—C10—H10A	108.6
C10—N2—Cu1	123.6 (2)	N2—C10—H10B	108.6
Cu1—N3—H3	98 (3)	N2—C10—C11	114.5 (3)
C14^{ii}—N3—Cu1	114.94 (18)	H10A—C10—H10B	107.6
C14^{ii}—N3—H3	109 (3)	C11—C10—H10A	108.6
C13—N3—Cu1	116.87 (19)	C11—C10—H10B	108.6
C13—N3—C14^{ii}	109.7 (2)	C2—C7—H7	118.7
C13—N3—H3	108 (3)	C6—C7—C2	122.6 (3)
C1—N1—Cu1	124.4 (2)	C6—C7—H7	118.7
C1—N1—C12	115.6 (3)	C5^{i}—C6—C7	116.9 (3)
C12—N1—Cu1	119.8 (2)	C5^{i}—C6—C8	121.6 (4)
N3^{ii}—C14—H14A	109.0	C7—C6—C8	121.5 (4)
N3^{ii}—C14—H14B	109.0	C12—C11—C10	113.7 (4)
N3^{ii}—C14—C13	112.8 (3)	C12—C11—H11A	108.8
H14A—C14—H14B	107.8	C12—C11—H11B	108.8
C13—C14—H14A	109.0	C10—C11—H11A	108.8
C13—C14—H14B	109.0	C10—C11—H11B	108.8
O1—C3—C4^{i}	121.2 (2)	H11A—C11—H11B	107.7
O1—C3—C2	121.5 (3)	C6—C8—H8A	109.5
C2—C3—C4^{i}	117.3 (3)	C6—C8—H8B	109.5
C4—C5—H5	118.2	C6—C8—H8C	109.5
C6^{i}—C5—H5	118.2	H8A—C8—H8B	109.5
C6^{i}—C5—C4	123.6 (3)	H8A—C8—H8C	109.5
C3^{i}—C4—C9	125.0 (3)	H8B—C8—H8C	109.5
C5—C4—C3^{i}	119.5 (3)		

Symmetry codes: (i) $-x$, $-y + 1$, $-z-1$; (ii) $-x$, $-y$, $-z-1$

displaced by 0.083(6) Å from the planar equatorial donor atoms N_2O_2 toward H_2O. The mode of coordination of Cu2 to the square plane N_2O_2 atoms is similar to Cu1 in the hexa-coordinated molecule. Typical equatorial bond lengths and angles are: Cu2–O = 1.970(6) Å, Cu2–N = 1.943(9) Å, *cis* O–Cu2–N = 93.9(3)° and *tran* O–Cu2–N 168.1(3)°. All equatorial bond lengths are shorter and the apical distances are longer than the ones found in our report, consistent with a stronger Jahn–Teller effect in the presence of weaker ligands, H_2O and perchlorate ion when compared to piperazine.

More recently we described the crystal structure of the coordination polymer $[\{Cu_2(tidf)(H_2O)\}_2(\mu\text{-}CN)_2Fe(CN)_4]\cdot 6H_2O$. In this case, the pentacoordinated copper(II) units $[Cu_2(tidf)(H_2O)]^{2+}$ are linked by a hexacyanoferrate(II) ion through two cyano–bridges in a *trans* configuration and the unit cell revealed a complex supramolecular structure sustained by hydrogen-bond interactions between the metallo–complex and the crystallization water molecules [7].

An extended 1D architecture along the crystallographic axis *b* for complex $[\{Cu_2(tidf)(\mu\text{-}ppz)\}(ClO_4)_2]_n$ is shown in the packing, Fig. 2. The complex also expands in the *ac* crystallographic plane in a supramolecular tridimensional assembly through weak hydrogen bonds with the perchlorate

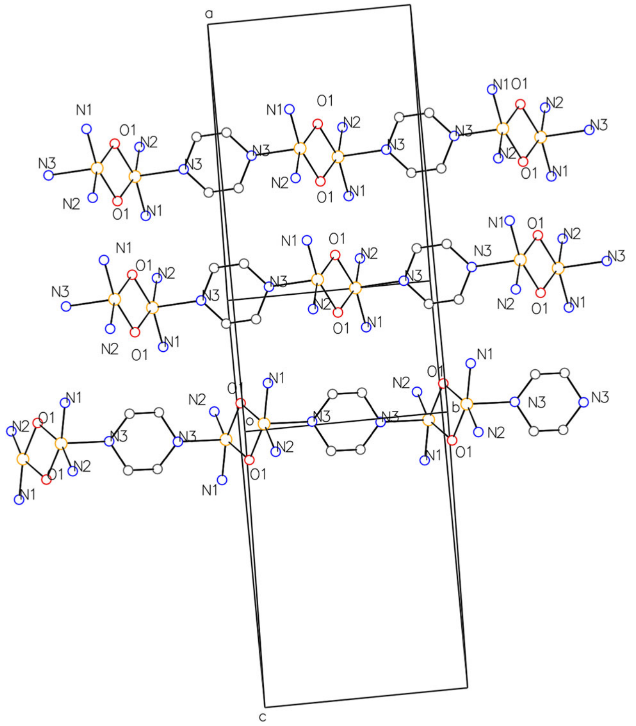

Fig. 2 View of the chain structure of $\{Cu_2(tidf)(\mu\text{-}ppz)\}(ClO_4)_2]_n$, along the crystallographic *ab* plane

Table 3 Hydrogen-bonding geometric parameters (in Å and °) for $[\{Cu_2(tidf)(\mu\text{-}ppz)\}(ClO_4)_2]_n$

D—H···*A*	*D*—H	H···*A*	*D*···*A*	*D*—H···*A*
N3—H3···O13^{i}	0.88 (2)	2.60 (3)	3.386 (5)	149 (3)
N3—H3···O11^{i}	0.88 (2)	2.36 (2)	3.183 (4)	156 (3)
C5—H5···O14^{iii}	0.93	2.45	3.330 (5)	158
C10—H10*B*···O12^{iv}	0.97	2.35	3.274 (6)	159
C7—H7···O12^{v}	0.93	2.60	3.460 (5)	154
C11—H11*B*···O14	0.97	2.69	3.406 (6)	131
C8—H8*A*···O13^{vi}	0.96	2.62	3.331 (6)	131

Symmetry codes: (i) $-x+1$, $-y+1$, $-z+1$; (iii) $-x+2$, $-y+1$, $-z+1$: (iv) x, $y-1$, z; (v) $-x+3/2$, $y-1/2$, $-z+3/2$; (vi) $x-1/2$, $-y+3/2$, $z+1/2$

ion, like C10–H10B···O12^{iv} and C8-H8A···O13^{vi} (iv = x, $y-1$, z; vi = $x+1$, $-y+3/2$, $z+1/2$) at 3.274(6) Å and 3.331(6) Å for D…A distance. The N3 atom of piperazine is participating as donor in two hydrogen bonds with oxygen atoms of perchlorate. The corresponding geometrical parameters are given in Table 3.

Infrared Spectra

The infrared spectrum of $[\{Cu_2(tidf)(\mu\text{-}ppz)\}(ClO_4)_2]_n$ showed bands also observed in the related complex $[Cu_2(tidf)(ClO_4)_2(H_2O)_2]$, but at different wavenumbers. Main bands are at 1641 ν(C = N), 1,568 ν(C = C) and 1,326 ν(C–O) cm^{-1}, characteristic of the tetraiminodiphenolate macrocycle. Piperazine exhibited the typical ν(N–H) mode at 3,284 cm^{-1}, while bands at 561 and 524 cm^{-1} were accounted to the vibrational modes νCu–N and νCu–O, respectively. Values seen for the parent complex, $[Cu_2(tidf)(ClO_4)_2(H_2O)_2]$, for νCu–N and νCu–O were 594 and 519 cm^{-1} and consistent with the effect of the axial coordination of the piperazine to the copper(II) ion. Perchlorate ion presented typical bands at 1,095 and 622 cm^{-1}.

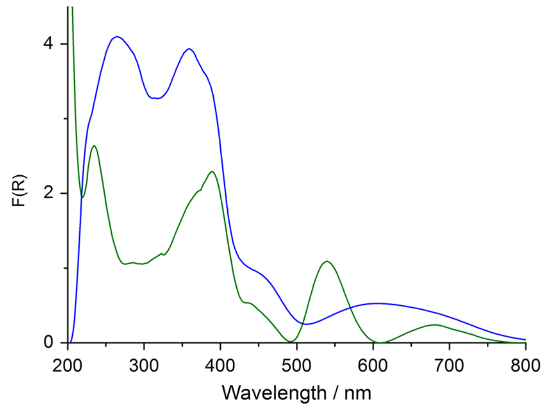

Fig. 3 Diffuse reflectance spectrum of $[\{Cu_2(tidf)(\mu\text{-}ppz)\}(ClO_4)_2]_n$ (*green line*) and comparison with the related complex, $[Cu_2(tidf)(ClO_4)_2(H_2O)_2]$ (*blue line*) (Color figure online)

UV–vis Spectra

Figure 3 shows the UV–visible spectrum of a solid sample of complex $[\{Cu_2(tidf)(\mu\text{-}ppz)\}(ClO_4)_2]_n$ (green line) along with the spectra of the related complex $[Cu_2(tidf)(ClO_4)_2(H_2O)_2]$. The bands in the 200–400 nm range are mainly intra-ligand π(tidf) → π*(tidf) transitions, which are also observed in the spectrum of the free macrocyclic ligand. A metal-to-ligand charge transfer $d_\pi(Cu^{II})$ → p_π tidf transition was assigned to the band at 450 nm.

Complex $[Cu_2(tidf)(ClO_4)_2(H_2O)_2]$ shows a broad structure-less band centered at 605 nm, typical of copper(II) in a D_{4h} ligand field symmetry and has contributions from three d–d transitions, $z^2 \rightarrow x^2{-}y^2$, $xy \rightarrow x^2{-}y^2$ and $(xz, yz) \rightarrow x^2{-}y^2$ [29]. This band splits in the spectrum of $[\{Cu_2(tidf)(\mu\text{-}ppz)\}(ClO_4)_2]_n$ (green line) at 540 and 680 nm, reflecting the different geometries around the copper(II) ions in both compounds. The lower energy component of the d–d transition for $[\{Cu_2(tidf)(\mu\text{-}ppz)\}(ClO_4)_2]_n$ can be explained using crystal-field arguments. Here, copper(II) is in a C_{4v} symmetry and it is equivalent of an infinite elongation of one of the axial ligands, reducing the repulsions along the *z* direction. As a result, a new set of energies is established for the metal orbitals and the d–d bands are shifted, particularly the

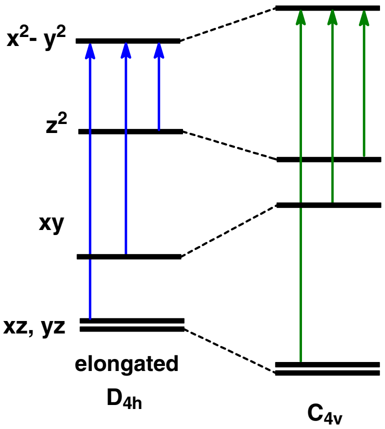

Scheme 2 Crystal-field orbital splittings of [{Cu_2(tidf)(μ-ppz)}(ClO_4)$_2$]$_n$

higher energy (xz, yz) → x^2-y^2 transition as represented in Scheme 2. The other two transitions z^2 → x^2-y^2 and xy → x^2-y^2 are overlaid [7].

Conclusion

The coordination polymer [{Cu_2(tidf)(μ-ppz)}(ClO_4)$_2$]$_n$ was prepared from the reaction between [Cu_2(tidf)(ClO_4)$_2$(H_2O)$_2$] and piperazine (1:1 molar ratio) in a water/isopropanol/acetonitrile mixture. Structural analysis showed square pyramidal copper(II) ions covalently bridged by piperazine. Some intermolecular interactions by hydrogen bonding complete the molecular arrangement at the solid state. The electronic structure of the compound is sensitive to the geometry around the copper and the spectra can be correlated with the degree of tetragonal distortion.

Supporting Information Available

CCDC-1008584 contains the supplementary crystallographic data for this paper. These data can be obtained free of charge at www.ccdc.cam.ac.uk/conts/retrieving.html [or from the Cambridge Crystallographic Data Centre (CCDC), 12 Union Road, Cambridge CB2 1EZ, UK; fax: +44(0)1223-336033; email: deposit@ccdc.cam.ac.uk].

Acknowledgments F.S.N. and M.A.R. thank CNPq and CAPES for research fellowships. Diffractometer was supported by the CAPES – Pró-Equipamentos 024/2012 and visiting professor program A0099/2013.

References

1. Hakimi M, Moeini K, Mardani Z, Mohr F (2014) Polyhedron 70:92–100
2. Vaddypally S, Xu C, Zhao S, Fan Y, Schafmeister C, Zdilla MJ (2013) Inorg Chem 52:6457–6463
3. Kim E, Lee H (2013) Inorg Chim Acta 399:62–66
4. James L, Kose M, Metcalfe T, McKee V (2011) J Chem Crystal 41:577–581
5. Nunes FS, Murta PDL, da Cunha CJ (1999) J Coord Chem 47:251–267
6. Robson R, Pilkington NH (1970) Aust J Chem 23:2225–2236
7. Samulewski RB, Rocha JC, Stieler R, Lang ES, Evans DJ, Poneti G, Nascimento OR, Ribeiro RR, Nunes FS (2011) Polyhedron 30:1997–2006
8. Samulewski RB, Rocha JC, Fuganti O, Stieler R, Lang ES, Vaz MGF, Nunes FS (2010) J Mol Struct 984:354–358
9. Raimondi AR, Evans DJ, Nunes FS (2008) Spectrochim Acta A 70:651–654
10. Raimondi AR, Evans DJ, Drechsel SM, Hasegawa T, Nunes FS (2007) Spectrochim Acta A 67:145–149
11. Raimondi AC, Hasegawa T, Evans DJ (2005) Spectrochim. Acta A 61:1929–1932
12. Raimondi AC, Hitchcock PB, Leigh GJ, Nunes FS (2004) J Chem Crystal 34:83–87
13. Raimondi AC, Mangrich AS, Franco VS, Toma HE, Nunes FS (2004) Polyhedron 23:2069–2074
14. Raimondi AC, Hitchcock PB, Leigh GJ, Nunes FS (2002) J Chem Crystal 32:363–367
15. Thompson LK, Mandal SK, Tandon SS, Bridson JN, Park MK (1996) Inorg Chem 35:3117–3125
16. Gagné RR, Spiro CL, Smith TJ, Hamann CA, Thies WR, Shiemke AK (1981) J Am Chem Soc 103:4073–4081
17. Spiro CL, Lambert LL, Smith TJ, Duesler EN, Gagné RR, Hendrickson DN (1981) Inorg Chem 20:1229–1237
18. Gagné RR, Henling LM, Kistenmacher TJ (1980) Inorg Chem 19:1226–1231
19. Lambert SL, Hendrickson DN (1979) Inorg Chem 18:2683–2686
20. Okawa H, Kida S (1972) Bull Chem Soc Jap 45:1759–1764
21. Ishiruji FHO, Evans DJ, Benedito FL, Nunes FS (2008) Spectrochim Acta A 70:1029–1033
22. Atanasov M, Comba P, Hausberg S, Martin B (2009) Coord Chem Rev 253:2306–2314
23. Paraschiv C, Andruh M, Journaux Y, Zak Z, Kyritsakas N, Ricard L (2006) J Mater Chem 16:2660–2668
24. Mandal SK, Thompson LK, Newlands MJ, Gabe EJ (1989) Inorg Chem 28:3707–3713
25. Mohanta S, Nanda KK, Ghosh S, Mukherjee M, Heliwell M, Nag K (1996) J Chem Dalton Trans 22:4233–4238
26. Sheldrick GM (2008) Acta Cryst. A64:112–122
27. Johnson CK (1970b) Crystallographic Computing, Ahmed FR, Hall SR, Huber CP (eds) pp. 207–219. Copenhagen: Munksgaard
28. Dolomano OV, Bourhis LJ, Gildea RJ, Howard JAK, Puschmann H (2009) OLEX2: a complete structure solution, refinement, analysis program. J Appl Cryst 42:339–341
29. Protasiewyck G, Nunes FS (2006) Spectrochim Acta A 65:549–552